Results in Physics 13 (2019) 102218

Contents lists available at ScienceDirect

Results in Physics

journal homepage: www.elsevier.com/locate/rinp

Investigation of optical and electrical properties of Cobalt-doped Ge-Sb-S thin film

Ishaq Musa[a,*], Zaid Qamhieh[b], Saleh Mahmoud[c], Mohamad El-Shaer[d], Ahmad Ayesh[d], Naser Qamhieh[c]

[a] Department of Physics, Palestine Technical University– Kadoorie, P.O. Box 7, Tulkaram, Palestine
[b] Department of Physics, An-Najah National University, Nablus, Palestine
[c] Department of Physics, UAE University, P.O. Box 17555, Al-Ain, United Arab Emirates
[d] Department of Mathematics, Statistics and Physics, Qatar University, P.O. Box 2713, Doha, Qatar

ARTICLE INFO

Keywords:
Amorphous chalcogenides
Cobalt doping
Optical band gap
Raman spectroscopy
Capacitance measurements

ABSTRACT

Amorphous Germanium Antimony Sulphide (Ge-Sb-S) doped with Cobalt (Co) have been deposited on glass substrates by thermal evaporation technique on a glass substrate. The films deposited onto glass substrates are characterized by Energy Dispersive X-ray Fluorescence Spectrometer, UV–VIS spectrophotometer, Raman spectroscopy, and Capacitance-Voltage Keithley meter. The optical band gap was calculated from the UV–Visible spectrum and found to be 2.05 eV. Raman spectroscopy measurements reveal that a wide band spectrum from 300 to 410 cm^{-1} centered at 355 cm^{-1}. The Raman shift peaks at 325 cm^{-1} and 350 cm^{-1} are as-signed to the bond stretching mode Sb-S and Ge-S, respectively. In addition, from the obtained Raman spectra it is concluded that the presence of Co doped with Ge-Sb-S. The capacitance and conductance versus voltage measurements were performed at different temperatures. The results show a slight increase in the capacitance with temperature and it reaches a maximum value around 150 °C, and eventually it becomes negative. This behavior is interpreted in terms of the nucleation growth process and the thermally activated conduction process with measured activation energy of 0.79 eV.

Introduction

Due to their numerous applications in several fields, chalcogenide materials have received appreciable consideration for fundamental research [1–4]. These materials have become of interest in memory devices after 1960's when Ovshinski suggested a reversible and rapid amorphous-crystalline phase change (PC) [5]. The switching between the two states can be accomplished either by light or by electrical pulses. Ternary Tellurium alloys such as Ge-Sb-Te are commonly used as active materials for electronic Pc memories [3,6,7]. In these materials, the transition between the two states occurs as they are heated up above crystalline temperature by a current pulse which is sufficiently applied to make the material crystallizes [8]. Crystallization in amorphous semiconductors occurs due to nucleation followed by growth processes [1,9]. At the beginning, crystalline nuclei are formed, then by increasing the temperature they grow up to form crystalline islands. The growth of the crystalline islands of the film is accomplished by varying some of its electrical properties such as capacitance [10]. It is found that the capacitance of Ge-Sb-Te is equivalent to a parallel plate capacitor of dimensions associated to the film thickness and the distance between the crystalline islands separated by a dielectric amorphous material.

The electrical conductivity of about 10^{-4} $(\Omega.cm)^{-1}$ for Ge-Sb-Te films allows the capacitance measurements to happen [10,11]. Although tellurium-based compounds such as Ge-Sb-Te films are the most popular phase change materials, scientists would like to avoid using them in all applications especially the production lines of memory devices due to their hazardous effects on the environment [12-14]. Some of the Tellurium (Te) free phase change materials such as Ge-Sb showed a limited crystal-growth [9]. Sulphur (S) is an alternative element to replace Tellurium (Te) in alloys such as $Ge_{30}Sb_{10}S_{60}$, which is widely studied [7,15–17]. For low power devices, the low conductivity of S based films of about 10^{-9} $(\Omega.\ cm)^{-1}$ and consequently, the low possible current is not sufficient to heat and activate the material to perform an amorphous- crystalline phase transformation. It is reported that alloying $Ge_{30}Sb_{10}S_{60}$ with transition elements such as Cobalt atoms enhances the electrical conductivity by few orders of magnitude [15], and reduces the optical gap towards lower energy values [18]. In this work,

* Corresponding author.
E-mail address: i.musa@ptuk.edu.ps (I. Musa).

https://doi.org/10.1016/j.rinp.2019.102218
Received 15 February 2019; Received in revised form 20 March 2019; Accepted 20 March 2019
Available online 23 March 2019

we investigate the optical band gap and Raman spectroscopy of Ge-Sb-S doped with Cobalt. Also, we study the variation of capacitance and conductance of thin films.

Experimental

Thermal evaporation process was used to form thin films of about 1 μm thickness onto glass substrate of melt- quenched glasses of the $Ge_{30}Sb_{10}S_{60}$ + Co. Thermal evaporation is the standard and most popular technique used for depositing chalcogenide materials. It is popular for chalcogenides due to their relatively law melting point, and it is ultimately the cheapest and can still provide sufficient thin film deposition with high purity. The chemical composition of the prepared thin films was determined by Energy Dispersive X-ray Fluorescence Spectrometer (Shimadzu 7000). The optical absorption spectra were obtained using Jasco UV–Visible spectrophotometer. In order to get the phonon vibrational study of the $Ge_{30}Sb_{10}S_{60}$ doped by Co, the XploRA ONE Raman microscope from Horiba, with 765 nm excitation laser light, was used to carry out Raman spectroscopy measurements. The electrical contacts were connected to two parallel gold electrodes which were evaporated on the top of a glass substrate followed by film deposition and producing an active area of 1 × 1 mm^2. The capacitance-voltage and the conductance measurements were done by the help of 590 CV Keithley meters which operates at 100 kHz frequency. The measurements were done for different temperatures, and for each temperature the voltage was swept from −20 to +20 V. However, the temperature of the sample was measured by a K-type thermocouple, and it was increased at a rate of 10 °C/min inside argon gas to avoid oxidation.

Results and discussion

EDX Fluorescence Spectrometer analysis

Fig. 1 shows the chemical composition of the prepared thin films measured by Energy Dispersive X-ray Fluorescence Spectrometer. In the picture, the colored concentric circles represent the different collimator sizes that can be used to focus on the sample, such as 1 mm, 3 mm, 5 mm, and 10 mm. One can choose different collimator size to focus on the sample and it will give the elemental composition in that particular region. The green colored ring represents the collimator which has been chosen for the analysis in Fig. 1, which has 5 mm diameter. The elemental atomic percentage in the thin film was found to be

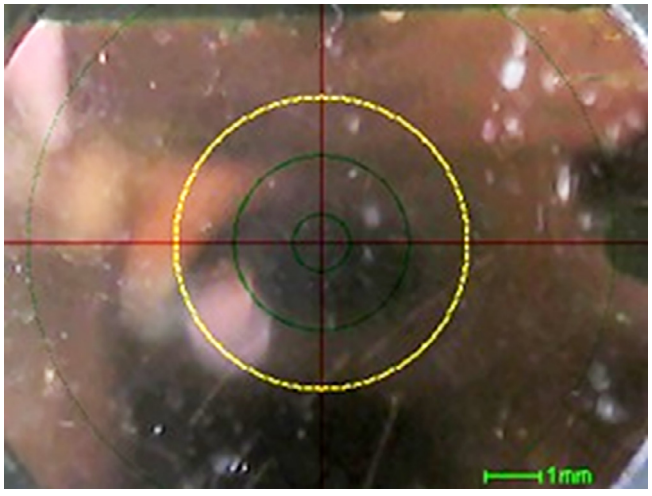

Fig. 1. Thin film of $Ge_{30}Sb_{10}S_{60}$ doped with Co measured by Energy Dispersive X-ray Fluorescence Spectrometers. The element atomic percentage in the thin films was found to be Ge = 18.99%, Sb = 16.91%, S = 63.99%, and Co = 0.12%.

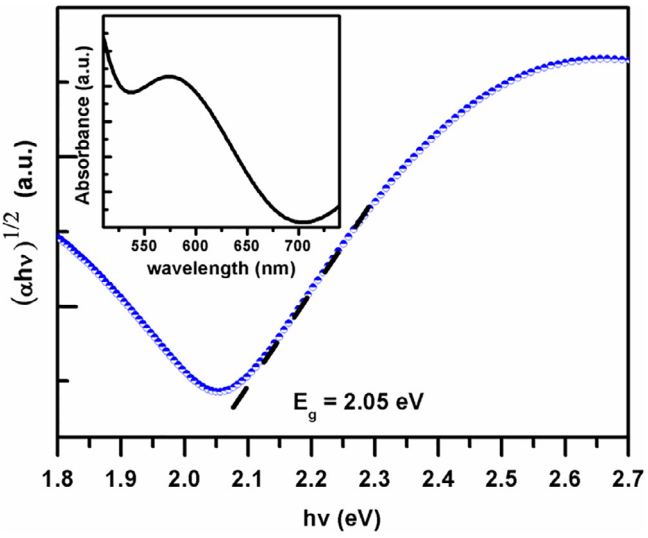

Fig. 2. $(\alpha hv)^{1/2}$ against the photon energy (hv) for the film. The intercept of the dashed line with the energy axis gives the energy band gap of the alloy.

$Ge_{18.99}Sb_{16.91}S_{63.99}Co_{0.12}$. The difference in the composition of the film from the melt-quenched glass is due to the difference in the melting point of the constituents in the precursor compound.

UV–Vis absorption and optical band gap

Optical absorption measurement is a widely used technique to characterize the electronic properties of materials, through the determination of the parameters describing the electronic transitions. The analysis of the ultraviolet/visible absorption spectrum of the thin films provides information about the absorption coefficient α, and the band gap can be deduced. A widespread model used to determine the optical properties of amorphous semiconductors is the Tauc model [19]. It's a plot of the square root of the product of α and the energy of the absorbed light $(\alpha hv)^{1/2}$ against the photon energy (hv) where h is Planck's constant and v is the frequency of the absorbed light. The Tauc plot of thin film $Ge_{18.99}Sb_{16.91}S_{63.99}Co_{0.12}$, is shown in Fig. 2, and the inset Fig. 2 exhibits absorption edge at about 590 nm (2.1 eV). The optical band gap is determined from the crossing of the extrapolation of the linear part of the curve with the energy axis. The estimated value for the optical energy gap in the film is $E_g \cong 2.05\ eV$. Huang and coworkers showed that the optical band gap of Ge-Sb-S for different element atomic percentage composition of thin films between 2.16 and 2.58 eV [6]. The value of the optical band gap, 2.05 eV is less than finding in literature [6,17,20] and it can be attributed due to Co doping in Ge-Sb-S. It is reported that by introducing small amounts of metal, fraction of atomic percent, results in a minor change in optical energy gap [18].

Raman spectroscopy analysis

Fig. 3(a) and (b) shows Raman shift spectrum of Ge-Sb-S doped with Co that have been measured from 50 to 700 cm^{-1} with high and low power laser using density filter. The results show that the peaks of Raman spectrum at low power laser were clearly and give more information about the materials than the high power laser.

The broad band centered at about 355 cm^{-1} in Fig. 3(a). corresponds to the vibrational modes of heteropolar Ge-S and Sb-S bonds in the Sb2S3 tetrahedral and GeS2 pyramidal structural units [21]. These heteropolar bonding are more obvious in Fig. 3(b). at 325 cm^{-1} for Sb-S bonds and the shoulder at about 350 cm^{-1} for Ge-S bonds. Furthermore, the peaks around 425 and 447 cm^{-1} are due to the bond stretching of S-S (S8) which is very well known in Sulphur, whose

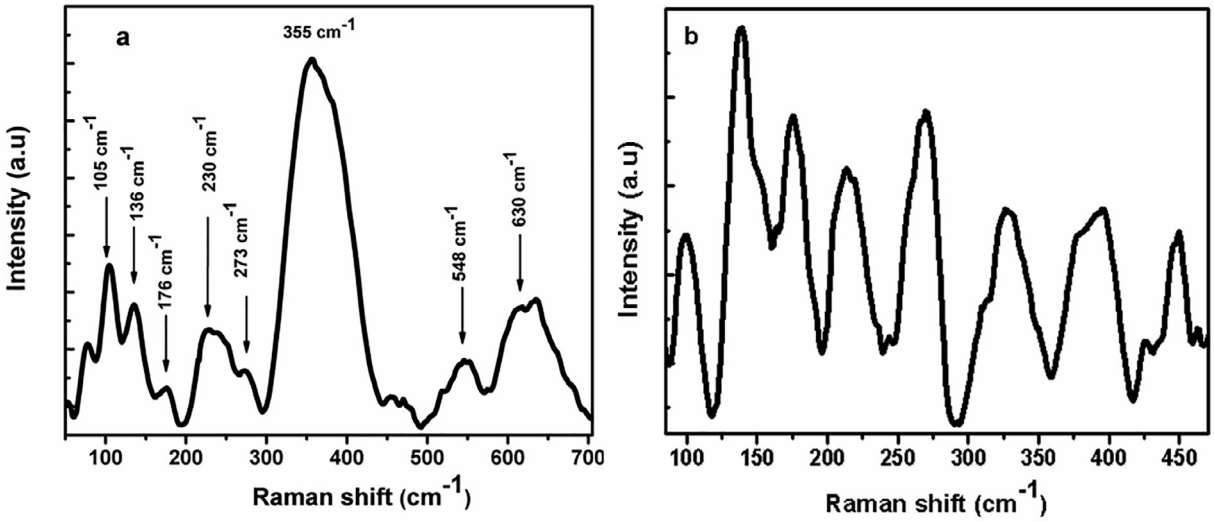

Fig. 3. Raman spectra of Ge-Sb-S doped with cobalt. The wavelength of the exciting laser beam used was 765 nm. (a) without density filter and (b) with density filter 0.1.

atoms are integrated into the film structure in the form of -S-S- group bridging [6,22]. At 219 cm^{-1} and 175 cm^{-1}, these Raman peaks belong to Ge-Ge homopolar and Sb-Sb bonding, respectively. It has been reported that two peaks appear in the spectra at 110 and 146 cm^{-1} when a Ge-Sb-S film is exposed to an energetic laser beam, and become more obvious in Ge-rich ternary alloys spectra. These two peaks are similar to that at 100 and 140 cm^{-1} of the spectrum in Fig. 3(b), and are attributed to the crystalline Sb [6]. Raman spectrum shown in Fig. 3(a). from 500 to 700 cm^{-1} also shows peaks centered at 548 and 630 cm^{-1} which did not appear in the reported Raman spectrum for pure Ge-Sb-S films [6,21]. The appearance of these peaks could be explained by the existence of cobalt bonding such as Co-S in the Co doping Ge-Sb-S films. It is worth noting that similar Raman shift peaks were observed in the spectrum of cobalt oxide and cobalt cement [23,24].

Electrical measurements

The capacitance of the thin films was measured as a function of temperature at 100 kHz frequency and applied potentials ranging from −20 to +20 Volts is shown in Fig. 4. At the beginning, the capacitance increases by an amount of 0.15 pF to its maximum value at about 150 °C. Beyond this temperature, the capacitance starts to decrease and it gets negative for temperatures above 230 °C. This behavior of the capacitance with temperature is similar to what was observed in $Ge_2Sb_2Te_5$ films [10]. Varying the applied potential has no remarkable effect on the measured capacitance of the thin films, which means that the capacitance is field independent at all temperatures except at 240 °C, where a shallow variation in the capacitance is observed. Using 590 CV Keithley meter in measuring the capacitance enables measuring the conductance (G) of the films simultaneously. In Fig. 5. the dependence of the conductance of the thin films is demonstrated as a function of the applied potential and at different temperatures. Similar to semiconductors, the conductance in the film increases with temperature. The conductance (G) versus the inverse of temperature (1/T) is shown in Fig. 6. From the slope of this figure, the calculated activation energy of about 0.79 eV is responsible for thermally activated conduction.

As the temperature in amorphous semiconductors increases, small crystalline nuclei are initially formed and then start to grow, in what is known as nucleation and growth process [25]. During this process, the nuclei grow in area and form crystalline islands separated by the amorphous medium as presented in Fig. 7. By increasing the temperature, the area of the crystals (A) increases and therefore, the separation

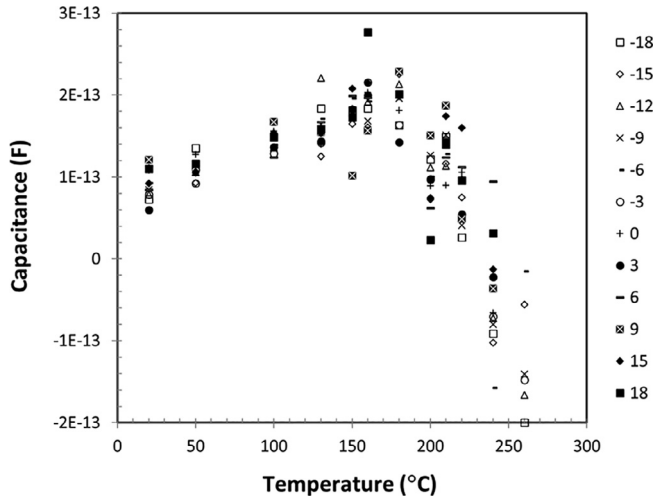

Fig. 4. Capacitance variation of the film as a function of temperature at different applied bias voltages, ranged from −20 to +20 V at 100 kHz frequency.

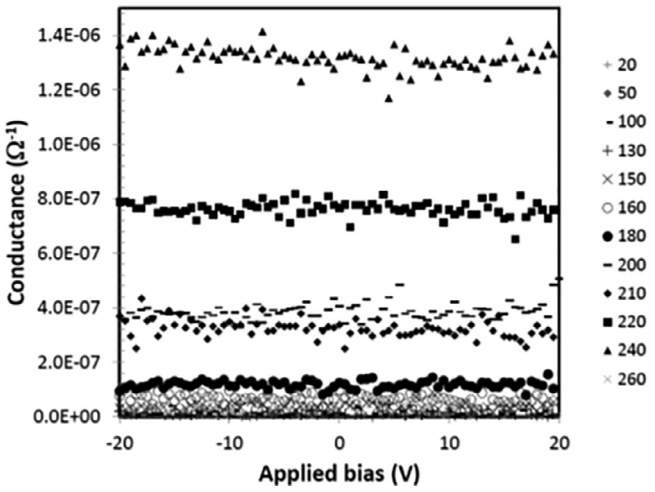

Fig. 5. The conductance of the film as a function of applied bias voltage (−20 V to +20 V) at different temperatures ranged from 20 to 260 °C. The frequency used is 100 kHz.

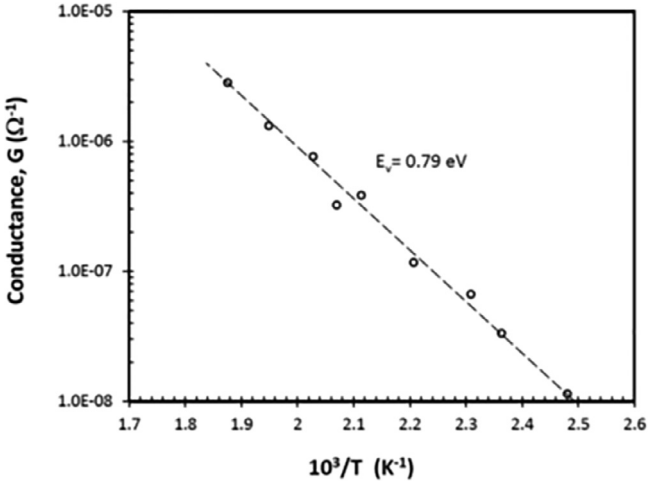

Fig. 6. The conductance-temperature dependence of the film.

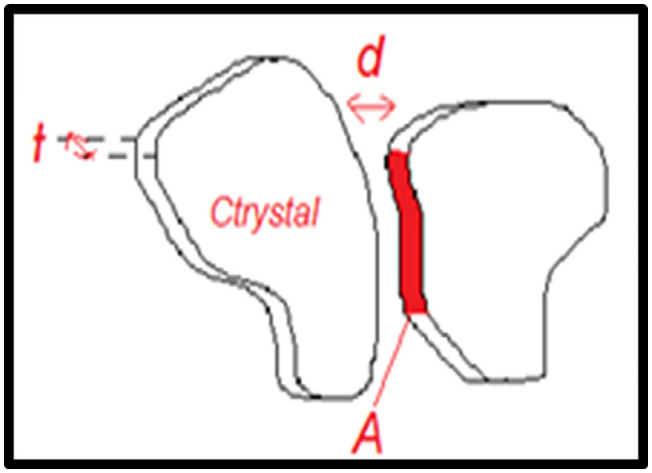

Fig. 7. A schematic drawing represents an adjacent crystalline islands embedded in amorphous matrix.

between them (d) decreases. The films composed of the crystalline islands surrounded by amorphous material can be considered as combination of capacitors connected in series and parallel. The equivalent capacitance (C) of such combination can be determined by measuring the capacitance of the thin film experimentally by the C-V meter with applying AC voltage across the film. In Fig. 5 the capacitance variation can be interpreted by Eq. (1):

$$C = \frac{A\varepsilon}{4\pi d}\left[1 - \frac{4\pi\tau\sigma}{\varepsilon(1+\omega^2\tau^2)}\right] \quad (1)$$

where, A is the thickness of the film, t, multiplied by the effective length of the crystalline island (the area of the plate capacitor) and d is the separation between the crystalline islands (dielectric thickness), τ is the dielectric relaxation time, ε is the dielectric constant, and $\sigma$is the dc conductivity of the amorphous material between the crystals [26]. At low temperature, the conductivity of the film is dominated by that of the amorphous and it is relatively low as shown in Fig. 4. In Eq. (1), the conductivity appears in the second term. Therefore, a low value produces in significant contribution to the capacitance, and then, the capacitance becomes:

$$C = \frac{A\varepsilon}{4\pi d} \quad (2)$$

The material is mainly amorphous at low temperature, while the crystalline part is small in size resulting in a relatively large separation (d) between crystals. Accordingly, a small value of the capacitance should be obtained by Eq. (2). However, increasing temperature will relocate the molecules and the atoms towards minimizing energy, where crystals nucleation and growth process starts. Growing in the crystalline size leads to an increase in the cross sectional area (A) and to a decrease in the crystal separation (d). Therefore, an increment in the measured value of the capacitance at low temperature can be considered as an indicator for crystallization to occur. The increase in the measured capacitance, 0.15 pF, is similar to that observed in Ge-Sb-Te films [10,27] which are considered as good phase change materials for memory devices. Other materials showed temperature independent capacitance where the crystallization process is growth-limited similar to that observed in Ge-Sb [9].

The capacitance in Eq. (1) is also affected by the conductivity of the film, which is altered by temperature as shown in Fig. 5. Here, the conductance (G) is the reciprocal of the resistance (R), therefore, $G = 1/R = \sigma A/l$. At a certain high conductivity value, the second term becomes more significant than before, that leads to a decrease in capacitance as the temperature increases. Therefore, at high temperatures above 150 °C, the capacitance decreases until it gets negative as shown in Fig. 4. Negative capacitance phenomena have been noticed in previous studies of other semiconductors such as $Ge_2Sb_2Te_5$ [27], Cd_3As_2 [28], $CdTe$ [29], and $CdSe$ [30].

The dependence of the conductance on temperature (Fig. 6) shows that the Cobalt doped Ge-Sb-S thin films is thermally activated according to the Arrhenius relation:

$$G = G_0 e^{-E_v/k_B T} \quad (3)$$

where G_o is a pre-exponential factor related to the material, E_v is the conduction activation energy, T is the temperature and k_B is the Boltzmann's constant. From the slope of Fig. 6, the calculated activation energy is 0.79 eV. It is very well known in semiconductors that this activation energy is measured from Fermi energy level (E_F) to a relevant band edge if one type of charge carriers dominates the electric conduction process.

In chalcogenide semiconductors, the Fermi level (E_F) is almost in the middle of the energy gap [31–33], and consequently, this optical band gap can be estimated to be twice the value of the activation energy. Herein, for Co doped Ge-Sb-S film, the optical energy gap $E_g = 2.05\ eV$ is slightly higher than $2E_F = 1.58\ eV$. It could be attributed by incorporating small amounts of Co doped in Ge-Sb-S film.

Conclusions

Using capacitance-voltage measurements for investigating the electrical properties of the thermally evaporated $Ge_{18.99}Sb_{16.91}S_{63.99}Co_{0.12}$ film provides an insight into the crystallization as a function of temperature. At low temperatures, crystallization occurs by nucleation and growth process similar to the most popular phase change material used in memory devices. At high temperatures the capacitance decreases and eventually it becomes negative. The conductance is field independent, and it increases exponentially with temperature with activation energy of $E_v = 0.79\ eV$. This value is less than half the optical gap, $E_g = 2.05\ eV$, measured from the optical absorption and the Tauc's model. Moreover, Raman analysis shows a wide band spectrum from 300 to 410 cm^{-1}, and others in the range 500–700 cm^{-1} that may correspond to Cobalt vibrational modes. Using low power laser beam for excitation allows defining significant peak positions at 325 cm^{-1} and 350 cm^{-1} for the bond stretching mode Sb-S and Ge-S, respectively.

Acknowledgements

This work is funded by the University Program for Advanced Research - United Arab Emirates University, (project no. 31S313).

References

[1] Wuttig M. Nat Mater 2005;4:265.
[2] Kumar Arun, Singh Vipenpal, Singh Harkawal, Sharma Pankaj, Goyal Navdeep. Physica B 2019;555(15):41–6.
[3] Singh Pravin Kumar, Sharma SK, Tripathi SK, Dwivedi DK. Results Phys 2019;12:223–36.
[4] Atyia HE, Fouad SS, Pankaj Sharma AS, Farid NA, Hegab J. Optoelectronic Adv M 2018;20(5–6):319–25.
[5] Ovshinsky SR. Phys Rev Lett 1968;21:1450.
[6] Huang CC, Wu CC, Knight K, Hewak DW. J Non-Cryst Solids 2010;356:281.
[7] Petit L, Carlie N, Adamietz F, Couzi M, Rodriguez V, Richardson KC. Mater Chem Phys 2006;97:64.
[8] Wuttig M, Yamada N. Nat Mater 2007;6:824.
[9] Qamhieh N, Mahmoud ST, Ayesh AI, Ghamlouche H. Physica Status Solidi (A) 2012;209:2476.
[10] Ghamlouche H, Mahmoud ST, Qamhieh N, Ahmed S, Al-Shamisi H. Phys Scr 2007;77:015701.
[11] Dzhurkov V, Fefelov S, Arsova D, Nesheva D, Kazakova L. J Phys: Conf Ser 2014;558:012046.
[12] Cabral C, Krusin-Elbaum L, Bruley J, Raoux S, Deline V, Madan A, et al. Appl Phys Lett 2008;93:071906.
[13] Cabral C, Chen KN, Krusin-Elbaum L, Deline V. Appl Phys Lett 2007;90:051908.
[14] Chen YC, Rettner CT, Raoux S, Burr GW, Chen SH, Shelby RM, et al. In: 2006 International Electron Devices Meeting (2006), pp. 1–4.
[15] Tichý L, Tichá H, Vlček M. Mater Lett 1991;12:261.
[16] Nagels P, Tichý L, Tichá H. J Non-Cryst Solids 1993;164–166:1187.
[17] Metwally HS. Physica B 2000;292:213.
[18] Márquez E, Wagner T, González-Leal JM, Bernal-Oliva AM, Prieto-Alcón R, Jiménez-Garay R, et al. J Non-Cryst Solids 2000;274:62.
[19] Tauc J. Amorphous and Liquid Semiconductors. New York: Plenum; 1974. p. 171.
[20] Song S, Carlie N, Boudies J, Petit L, Richardson K, Arnold CB. J Non-Cryst Solids 2009;355:2272.
[21] Kotsalas IP, Papadimitriou D, Raptis C, Vlcek M, Frumar M. J Non-Cryst Solids 1998;226:85.
[22] Kohoutek T, Yan X, Shiosaka TW, Yannopoulos SN, Chrissanthopoulos A, Suzuki T, et al. J Opt Soc Am B, JOSAB 2011;28:2284.
[23] Yang J, Liu H, Martens WN, Frost RL. J Phys Chem C 2010;114:111.
[24] Bøckman O, Østvold T, Voyiatzis GA, Papatheodorou GN. Hydrometallurgy 2000;55:93.
[25] Meinders ER, Mijiritskii AV, van Pieterson L, Wuttig M. Optical Data Storage: Phase-Change Media and Recording. Netherlands: Springer; 2006.
[26] Majeed Khan MA, Zulfequar M, Husain M. Physica B 2005;366:1.
[27] Mahmoud ST, Ghamlouche H, Qamhieh N, Ahmed S. J Non-Cryst Solids 2008;354:1976.
[28] Gould RD, Din M. Superficies y Vacio 1999;9:230.
[29] Ismail BB, Gould RD. in (1996), pp. 46–51.
[30] Oduor AO. PhD thesis, Keele University, UK, 1997.
[31] Mott NF, Davis EA. Electronic Processes in Non-Crystalline Materials, Clarendon Press; Oxford University Press, Oxford; New York, 1979.
[32] Qamhieh N, Mahmoud ST, Ghamlouche H, Benkhedir ML. J Optoelectronics Adv Mater 2008;10(10):1448–51.
[33] Krebs D, Raoux S, Rettner CT, Burr GW, Shelby RM, Salinga M, et al. J Appl Phys 2009;106:054308.